



HAL
open science

International Comparison Exercise for Biological Dosimetry after Exposures with Neutrons Performed at Two Irradiation Facilities as Part of the BALANCE Project

David Endesfelder, Ulrike Kulka, Martin Bucher, Ulrich Giesen, Guy Garty, Christina Beinke, Matthias Port, Gaetan Gruel, Eric Gregoire, Georgia Terzoudi, et al.

► **To cite this version:**

David Endesfelder, Ulrike Kulka, Martin Bucher, Ulrich Giesen, Guy Garty, et al.. International Comparison Exercise for Biological Dosimetry after Exposures with Neutrons Performed at Two Irradiation Facilities as Part of the BALANCE Project. *Cytogenetic and Genome Research*, 2023, 163 (3-4), pp.163 - 177. 10.1159/000530728 . irsn-04584571

HAL Id: irsn-04584571

<https://irsn.hal.science/irsn-04584571>

Submitted on 24 May 2024

HAL is a multi-disciplinary open access archive for the deposit and dissemination of scientific research documents, whether they are published or not. The documents may come from teaching and research institutions in France or abroad, or from public or private research centers.

L'archive ouverte pluridisciplinaire **HAL**, est destinée au dépôt et à la diffusion de documents scientifiques de niveau recherche, publiés ou non, émanant des établissements d'enseignement et de recherche français ou étrangers, des laboratoires publics ou privés.

Cytogenetic and Genome Research

Manuscript:	CGR-0-0-0
Title:	International comparison exercise for biological dosimetry after exposures with neutrons performed at two irradiation facilities as part of the BALANCE project
Authors(s):	David Endesfelder (Corresponding Author), Ulrike Kulka (Co-author), Martin Bucher (Co-author), Ulrich Giesen (Co-author), Guy Garty (Co-author), Christina Beinke (Co-author), Matthias Port (Co-author), Gaetan Gruel (Co-author), Eric Gregoire (Co-author), Georgia Terzoudi (Co-author), Sotiria Triantopoulou (Co-author), Elizabeth Ainsbury (Co-author), Jayne Moquet (Co-author), Mingzhu Sun (Co-author), Maria Jesus Prieto (Co-author), Mercedes Moreno Domene (Co-author), Joan-Francesc Barquinero (Co-author), Monica Pujol-Canadell (Co-author), Anne Vral (Co-author), Ans Baeyens (Co-author), Andrzej Wojcik (Co-author), Ursula Oestreicher (Corresponding author)
Keywords:	biological effectiveness, RENEB, biological dosimetry, dicentric chromosomes, neutrons
Type:	Research Article

1 **International comparison exercise for biological dosimetry after exposures**
2 **with neutrons performed at two irradiation facilities as part of the**
3 **BALANCE project**

4 David Endesfelder^a, Ulrike Kulka^a, Martin Bucher^a, Ulrich Giesen^b, Guy Garty^c,
5 Christina Beinke^d, Matthias Port^d, Gaëtan Gruel^e, Eric Gregoire^e, Georgia
6 Terzoudi^f, Sotiria Triantopoulou^f, Elizabeth A. Ainsbury^g, Jayne Moquet^g,
7 Mingzhu Sun^g, María Jesús Prieto^h, Mercedes Moreno Domene^h, Joan-Francesc
8 Barquineroⁱ, Monica Pujol-Canadellⁱ, Anne Vral^j, Ans Baeyens^j, Andrzej
9 Wojcik^{k,l}, Ursula Oestreicher^{a,*}

10 *^aDepartment of Effects and Risks of Ionising and Non-Ionising Radiation, Federal Office for*
11 *Radiation Protection (BfS), Oberschleißheim, Germany,*

12 *^bDepartment of Ionizing Radiation, Physikalisch-Technische Bundesanstalt (PTB),*
13 *Braunschweig, Germany*

14 *^cRadiological Research Accelerator Facility (RARAF), Columbia University, Irvington, New*
15 *York, USA*

16 *^dBundeswehr Institute of Radiobiology, Munich, Germany*

17 *^eInstitut de Radioprotection et de Sûreté Nucléaire (IRSN), PSE-Santé, SERAMED, LRAcc*
18 *Fontenay-aux-Roses, France*

19 *^fHealth Physics, Radiobiology & Cytogenetics Laboratory, National Centre for Scientific*
20 *Research "Demokritos", Athens, Greece*

21 *^gRadiation, Chemicals and Environmental Hazards Directorate, UK Health Security Agency,*
22 *Chilton, Oxfordshire, UK*

23 ^h*Centro de Oncología Radioterápica, Laboratorio de dosimetría biológica, Hospital General*
24 *Universitario Gregorio Marañón, Madrid, Spain*

25 ⁱ*Departament de Biologia Animal, Unitat d'Antropologia Biològica, Universitat Autònoma de*
26 *Barcelona, Bellaterra, Catalonia, Spain.*

27 ^j*Faculty of Medicine and Health Sciences, Department of Human Structure and repair,*
28 *Radiobiology Research Unit, Ghent University, Gent, Belgium*

29 ^k*Department of Molecular Biosciences, The Wenner-Gren Institute, Stockholm University,*
30 *Stockholm, Sweden*

31 ^l*Institute of Biology, Jan Kochanowski University, Kielce, Poland*

32

33 ***Corresponding author:**

34 Dr. Ursula Oestreicher

35 Department of Effects and Risks of Ionising and Non-Ionising Radiation

36 Federal Office for Radiation Protection

37 Ingolstaedter Landstraße 1

38 85764 Oberschleissheim,

39 Germany

40 email: uoestreicher@bfs.de

41 phone number: +49 30 18333 2213

42 **Running Title:** The BALANCE project: Biological dosimetry after exposures with neutrons

43 **Number of Tables:** 3

44 **Number of Figures:** 4

45 **Word count:** 6186

46 **Keywords:** biological dosimetry, RENEB, neutrons, dicentric chromosomes, biological
47 effectiveness

48 **Abstract**

49 In the case of a radiological or nuclear event, biological dosimetry can be an important tool to
50 support clinical decision-making. During a nuclear event, individuals might be exposed to a
51 mixed field of neutrons and photons. The composition of the field and the neutron energy
52 spectrum influence the degree of damage to the chromosomes. During the transatlantic
53 BALANCE project, an exposure similar to a Hiroshima-like device at a distance of 1.5 km from
54 the epicenter was simulated and biological dosimetry based on dicentric chromosomes was
55 performed to evaluate the participants ability to discover unknown doses and to test the
56 influence of differences in neutron spectra. In a first step, calibration curves were established
57 by irradiating blood samples with 5 doses in the range of 0 Gy to 4 Gy at two different facilities
58 in Germany (PTB) and USA (CINF). The samples were sent to eight participating laboratories
59 from the RENEB network and dicentric chromosomes were scored by each participant. Next,
60 blood samples were irradiated with 4 blind doses in each of the two facilities and sent to the
61 participants to provide dose estimates based on the established calibration curves. Manual and
62 semi-automatic scoring of dicentric chromosomes were evaluated for their applicability to
63 neutron exposures. Moreover, the biological effectiveness of the neutrons from the two
64 irradiation facilities was compared. The calibration curves from samples irradiated at CINF
65 showed a 1.4 times higher biological effectiveness compared to samples irradiated at PTB. For
66 manual scoring of dicentric chromosomes, the doses of the test samples were mostly
67 successfully resolved based on the calibration curves established during the project. For semi-
68 automatic scoring, the dose estimation for the test samples was less successful. Doses >2 Gy in
69 the calibration curves revealed non-linear associations between dose and dispersion index of
70 the dicentric counts, especially for manual scoring. The differences in the biological
71 effectiveness between the irradiation facilities suggested that the neutron energy spectrum can
72 have a strong impact on the dicentric counts.

73

74 **Introduction**

75 In principle, various scenarios of large-scale radiological incidents are conceivable, ranging
76 from a fire to an explosion in a nuclear power plant, a dirty bomb an improvised nuclear device
77 (IND) or the detonation of a military grade nuclear weapon. In all these cases, a large number
78 of individuals are potentially exposed to ionizing radiation (Buddemeier and Dillon 2009) and
79 a quick and reliable dose assessment should be an essential part of radiation emergency
80 management. In the case of a nuclear disaster, the high number of injured or worried-well will
81 exceed the capacity of emergency preparedness of a single country. An effective strategy to
82 enhance analysis capacity in the case of large-scale accidents is networking between
83 experienced laboratories (Kulka et al. 2018). In Europe, the RENEb association (RENEb e.V.),
84 a network for biological dosimetry and physical retrospective dosimetry was founded in 2017
85 to act as a legal partner for organizations and platforms, active in emergency preparedness,
86 radiation protection and research (Kulka et al. 2016). The network provides rapid,
87 comprehensive and standardized methodology for individualized dose estimation in the case of
88 large-scale radiological events. Another strategy, RABiT (Rapid Automated Biodosimetry
89 Tool), was developed at Columbia University and is a tool that was designed to allow fully
90 automated analysis from the input of the blood samples into the machine to the output of a dose
91 estimate (Garty et al. 2010). This was combined with newer approaches using commercially
92 available High Throughput/High Content Screening platforms (Repin et al. 2017; Royba et al.
93 2019). The RABiT allows a high throughput processing of blood samples and dose estimates
94 with minimal need for manpower. Both approaches have strengths and weaknesses, but could
95 ideally complement each other, depending on the emergency scenario. This publication focuses
96 on the project results based on the RENEb networking approach and the project results on the
97 RABiT system will be published separately in later publications. Currently, the most qualified
98 methods for biological dosimetry are based on cytogenetic biomarkers in human peripheral
99 blood lymphocytes, such as dicentric chromosomes and micronuclei. These biomarkers have

100 already been validated in various radiation incidents in which they proved to be reliable tools
101 to detect an absorbed dose with sufficient precision (Beinke et al. 2015; Güçlü 2021; Salassidis
102 et al. 1994; Tawn et al. 2018; Wernli et al. 2015). In biological dosimetry, the dose received
103 by an individual is estimated based on an *ex vivo* calibration curve which is prepared by each
104 laboratory in advance. Calibration curves should be established for a range of radiation types
105 with different biological effectiveness.

106

107 Following a nuclear detonation, people are exposed to a mixed field of neutrons and gamma-
108 rays. In particular, in an IND scenario where the device is detonated at or near ground level,
109 the higher shielding of photons, compared to neutrons, by construction material will result in
110 an increased fraction of the dose delivered by neutrons (Kramer et al. 2016). Additionally, the
111 composition and energy distribution of the radiation field will depend on the distance from the
112 epicenter and shielding. As an example, at a distance of 1.5 km from the epicenter of a
113 Hiroshima-like device, the delivered dose is significant but survivable (Kramer et al. 2016). In
114 this case, the neutron energy spectrum is a relatively broad energy distribution peaking at
115 around 1 MeV but spanning energies from thermal up to about 10 MeV (Egbert et al. 2007)
116 and is markedly different from a standard reactor spectrum of fission neutrons (Garty et al.
117 2017; Xu et al. 2015b). Currently, most research on the relative biological effectiveness (RBE)
118 of neutrons with regard to the formation of dicentric chromosomes has been performed for
119 different energies of monoenergetic neutrons, where the RBE showed a peak at approximately
120 0.4 MeV (Pandita and Geard 1996; Schmid et al. 2003; Tanaka et al. 1999), or for fission
121 neutrons from different types of reactors (Fajgelj et al. 1992; Schmid et al. 2008; Schmid
122 1998). There are also some publications exploring cytogenetic data based on irradiations with
123 neutrons with broad energy spectra comparable to a nuclear event from an A-bomb or an IND
124 (Dobson et al. 1991; Heimers et al. 2005, 2006) or from Hiroshima and Nagasaki survivors
125 (Bloom et al. 1966). Nevertheless, it is currently not clear how far differences in the neutron

126 energy spectrum and the composition of the mixed beam, as encountered after such an event,
127 influence the level of cytogenetic damage in exposed lymphocytes. Data published by (Sasaki
128 et al. 2006) suggested that the structure of the energy spectrum of fission neutrons has only
129 little effect on the chromosomal effectiveness. Recently, a facility has been developed (Xu et
130 al. 2015b) for simulating a neutron spectrum similar to the spectrum encountered at the
131 Hiroshima bombing at 1.5 km from the epicenter. Calibration curves and the RBE based on
132 the scoring of micronuclei (Xu et al. 2015b) and various transcriptomic (Broustas et al. 2018;
133 Mukherjee et al. 2019) and metabolomic (Laiakis et al. 2019; Laiakis et al. 2017) endpoints
134 have been evaluated. In the frame of biological dosimetry, where the dicentric chromosome
135 assay (DCA) is the gold standard that is routinely used to evaluate dose in accidental and
136 potential malicious exposures, it is essential that laboratories, such as those in the RENEB
137 network, have appropriate calibration curves available.

138

139 The BALANCE project was a transatlantic cooperation between the European RENEB network
140 and Columbia University in the United States. The main aim of the project was to simulate
141 exposures in a nuclear event, with a relevant neutron spectrum and to improve, validate and
142 compare different approaches to estimate doses based on biological markers. In the frame of
143 the project, blood was irradiated at two different neutron/gamma sources: The Columbia IND
144 Neutron Facility (CINF) at the Radiological Research Accelerator Facility, USA and the
145 neutron facility at Physikalisch-Technische Bundesanstalt (PTB), Germany, both mimicking
146 neutron spectra similar to the relevant spectrum. Irradiations at two different facilities with
147 slightly different compositions of the energy spectra enabled the comparison of the biological
148 effectiveness between the facilities. Irradiation at CINF yielded a neutron spectrum spanning
149 0.05-8 MeV (Xu et al. 2015a) with a photon component of approximately 18% and irradiation
150 at the PTB yielded a neutron spectrum spanning 0.1-8 MeV with a photon component of 10%.
151 During the first part of the project calibration curves were established by each participating

152 laboratory based on each of the two different mixed-radiation fields to test the sensitivity to
153 detect differences in the neutron energy spectra from CINF and PTB and to clarify if one
154 calibration curve is sufficient to estimate the dose absorbed by people exposed to slightly
155 different distributions of radiation energies and beam compositions. In the second part of the
156 project, four blind-coded samples were irradiated in each of the two facilities and again
157 distributed to the participating laboratories, to test the validity of the calibration curves
158 established in part one of the project. Irradiated blood samples from both facilities were
159 distributed among eight laboratories associated in the RENE network. Each participating
160 laboratory established calibration curves for samples irradiated at both facilities, enabling the
161 evaluation of differences in the scoring of dicentric chromosomes between the participating
162 laboratories as well as differences in the biological effectiveness of the neutron fields from the
163 two facilities. Manual and/or semi-automatic scoring of dicentric chromosomes was performed
164 by the participants and the performance of the two different scoring modes for exposures in the
165 different mixed fields was assessed by estimating doses from blind-coded samples.

166

167

168

169

170

171 **Material and Methods**

172

173 **Participating laboratories and tasks**

174 In the frame of this project blood samples were exposed *ex vivo* at two different neutron
175 irradiation facilities (PTB, Germany and CINF, USA). In the first part of the project calibration
176 curves were established following the irradiation procedure at both facilities. In the second part,
177 validation of these calibration curves was performed by dose estimation of blind-coded blood
178 samples irradiated at both facilities. The blood samples were sent to the Federal Office for
179 Radiation Protection (BfS), Germany and further processed. Eight partners of the European
180 RENE network were involved in the analysis of blood samples and provided results.

181

182 **Irradiation conditions of blood samples**

183 For irradiations at the PTB accelerator facility (PIAF) (Brede et al. 1980), the intense neutron
184 field with a broad energy distribution was produced by a deuteron beam of 3.4 MeV with beam
185 currents of up to 52 μA on a thick, water-cooled beryllium (Be) disc. The energy spectrum of
186 the neutron beam starts from very low energies and ranges up to approximately 8 MeV
187 (Meadows 1993). The beam charge on the Be target and the charge of a transmission ionization
188 chamber at the exit of the collimator served as neutron monitors. Before and after the irradiation
189 of the samples, the total dose to tissue per target charge was determined according to ICRU
190 recommendations (ICRU 1989) with a tissue-equivalent (A-150) gas ionization chamber
191 (EXRADIN, T2-#381). The chamber had been calibrated in the ^{60}Co reference field of PTB.
192 The photon component was determined with a Geiger-Müller counter (Type MX 163, Alrad
193 Inst., Surrey England) to $(10 \pm 2) \%$. The dose rate was around 1.2 Gy/h. Three blood-filled
194 tubes were irradiated simultaneously side-by-side (shown in Fig. 1a). A temperature of about
195 35°C was maintained during the irradiation by means of a heater plate and a Styrofoam box.

196 For irradiations at CINF, neutrons were generated by impinging a 28 μ A mixed proton/deuteron
197 beam with an energy of 5 MeV on a water-cooled 0.5 mm thick Be target on copper backing
198 (Materion, Brewster, NY)(Xu et al. 2015b). Prior to irradiation, dosimetry was performed using
199 a custom-built tissue equivalent proportional counter (Rossi et al. 1960) that was calibrated to
200 a NIST-traceable radium source. Because of the possible variation of the dose rate during the
201 experiment, a second tissue-equivalent gas ionization chamber, placed downstream of the
202 neutron target, was used as a monitor to halt the beam when the prescribed dose was reached.
203 Twelve 5 mL vacutainers were mounted on a Ferris wheel rotating around the Be target with
204 the samples at an angle of 60° to the primary beam position (shown in Fig. 1b). Dose rate at the
205 vacutainers was 3 Gy/h of neutrons with a concomitant photon dose of 0.6 Gy/h. During
206 irradiation, 3 tubes per dose were removed from the wheel (and replaced with water containing
207 tubes) when each of the prescribed doses was achieved.

208

209 The neutron fields of PTB and CINF are qualitatively compared in Figure 1c with the Hiroshima
210 field at 1.5 km from the epicenter. Shown are the neutron fluences multiplied by the tissue-
211 kerma factors (Malmer 2001), which correspond to the dose distribution as a function of neutron
212 energy. The curves are overlaid in arbitrary units for better comparison of differences in shape
213 and are, therefore, not to scale. The most important difference between the two irradiation
214 platforms is that PTB uses a pure deuteron beam, filtered through a dipole magnet, whereas
215 CINF uses the direct beam from the accelerator, containing protons, deuterons and molecular
216 ions. This has the effect of significantly broadening the CINF energy spectrum due to the low
217 energy neutrons generated by the Be(p,n) reaction, compared to Be(d,n), resulting in a large
218 excess of <1 MeV neutrons as seen in Figure 1c, which have a higher RBE (Pandita and Geard
219 1996; Schmid et al. 2003). The higher energy at CINF (5 MeV vs 3.4 MeV) also results in more
220 high energy neutrons.

221 Each neutron facility provided (i) five blood samples that were irradiated with doses in the
222 range of 0 Gy to 4 Gy (Table 1) for the establishment of calibration curves, (ii) three test
223 samples irradiated with blinded doses and (iii) one unirradiated control sample. For this
224 publication, the test samples were re-labeled in increasing order of the corresponding doses:
225 Blind 1 (0 Gy), Blind 2 (CINF: 0.6 Gy; PTB: 0.654 Gy), Blind 3 (CINF: 1.2 Gy; PTB: 1.61 Gy)
226 and Blind 4 (CINF: 2.4 Gy; PTB: 2.23 Gy). Blood from each test sample was provided to the
227 laboratories without knowing the reference doses before the analysis.

228

229 **Blood sampling and shipment of blood samples**

230 Human blood samples were collected by venipuncture in 10 mL heparinized tubes from a total
231 of 4 (one for each calibration curve and blind-coded test sample from each neutron facility)
232 healthy adult human volunteers. As in a real emergency, blood samples used for the set-up of
233 calibration curves were not from the same individuals as those used for blind-coded samples in
234 the validation procedure. The blood samples were fully anonymized and as such not traceable
235 to the individual participants. In Germany, blood samples from healthy adult donors were
236 obtained, in heparinized tubes (Sarstedt AG & Co. KG., Germany) by venipuncture by
237 physicians according to §15 of the code of medical ethics for physicians in Bavaria, Germany,
238 following the principles of the Declaration of Helsinki. In the US blood was collected under
239 Columbia University IRB protocol AAAS3035.

240 After irradiation, blood samples were kept for 2 h at 37 °C to allow DNA repair. Blood samples
241 irradiated at PTB were transported to BfS in temperature-controlled boxes (15-25°C) within 24
242 h. Blood samples irradiated at CINF were placed in a 22 °C passive temperature-controlled
243 shipper (CREDO Cube; Pelican Biothermal, Maple Grove, MN) and sent to BfS by express
244 service within 48 h.

245

246 **Processing of blood samples at BfS and scoring procedure**

247 At BfS, the cultivation and preparation of blood samples were performed according to standard
248 procedures (IAEA 2011; ISO19238 2014; Oestreicher et al. 2018). Whole blood (0.5 ml) was
249 transferred to culture tubes containing RPMI-1640 culture medium (Biochrom, Berlin)
250 supplemented with 10% FCS (Biochrom, Berlin), 2% PHA (Biochrom, Berlin) and antibiotics
251 (Biochrom, Berlin). For cell-cycle controlled scoring, long-term Colcemid treatment (Roche,
252 Mannheim) with a final concentration in culture of 0.08 µg/ml was added 24 h after culture set
253 up. Blood samples were cultured in total for 48 h. For each dose point 20 parallel cultures were
254 set up. The hypotonic treatment of cells was carried out with 75 mM KCl. Cells were then fixed
255 in methanol:acetic acid (3:1) three times. The suspension was stored in the freezer (-18°C)
256 before aliquots of fixed cells were sent to 7 RENEb partners in the EU (BIR, Germany;
257 UKHSA, UK; UAB, Spain; IRSN, France; SERMAS, Spain; UGent, Belgium and NCSRd,
258 Greece). The task of each RENEb partner (8 laboratories in total) was to prepare Giemsa
259 stained slides and manually analyze 1000 cells or 100 dicentric chromosomes per dose point to
260 establish a calibration curve (ISO19238 2014). In the case of semi-automated scoring (Romm
261 et al. 2013), laboratories were asked to score as many cells as possible. Scoring was performed
262 according to the standard and validated procedure of each particular laboratory.

263

264 For validation of the calibration curves based on blind-coded test samples, culturing,
265 preparation and distribution of blood samples were performed according to the same procedure
266 as for the calibration curves in the first part of the project. The task of each RENEb partner was
267 to prepare Giemsa stained slides and manually and/or semi-automatically analyze dicentric
268 chromosomes for dose estimation. For both scoring methods triage and full scoring mode were
269 applied. For manual scoring requirements were to analyze 50 cells or 30 dicentrics per dose
270 point (2 slides and 25 cells per slide) for triage mode and 500 cells or 100 dicentrics per dose

271 point (2 slides and 250 cells per slide) for full mode. For semi-automated scoring the detection
272 of dicentric chromosomes was performed on a software-based procedure, where 150 cells
273 should be captured for triage mode and 1500 or more cells for full mode.

274

275 *Statistical analysis*

276 The physical reference doses of samples irradiated at PTB were slightly updated after the
277 participants provided the calibration curve estimates. All calibration curves and dose estimates
278 for the test samples were therefore re-estimated after the participants provided their estimates.
279 As commonly accepted for high-LET exposures (IAEA 2011), the calibration curves were
280 estimated assuming a linear dose-effect relationship. The calibration curves were estimated
281 using generalized linear models (R function “glm”) with identity link. In a first step,
282 overdispersion was accounted for by using a quasi-Poisson glm model. If the estimated
283 dispersion of this model was ≤ 1 , a Poisson glm model was used instead. The doses and
284 corresponding 95% confidence intervals (CI) were estimated using the approach described in
285 Savage et al. (Savage and Papworth 2000). For the calculation of 95% CIs of the dose estimate,
286 overdispersion of the dicentric yields of the test samples was accounted for by using the
287 empirical standard deviation of the dicentric yield if the dispersion index $\delta > 1$ and the Poisson
288 standard deviation if $\delta \leq 1$. To test whether the observed overdispersion is significantly different
289 from 1, the U test was applied as described in (IAEA 2011) and results with $U > 1.96$ were
290 assumed to be significantly overdispersed ($P < 0.05$).

291 In order to evaluate the performance of the participating laboratories the ζ -score was used and
292 calculated as described in (ISO13528 2005):

$$293 \quad \zeta = \frac{D - D^*}{\sqrt{s_D^2 - s_{D^*}^2}}$$

294 where D is the dose estimated by the DCA, D^* is the physical reference dose, s_D is the estimated
295 standard deviation corresponding to D and s_{D^*} is the standard deviation of the physical
296 reference dose. The standard deviation s_D was calculated as described in Savage et al. (Savage
297 and Papworth 2000), accounting for overdispersion of the test samples as described above. It
298 was assumed that s_{D^*} is small relative to s_D and was set to $s_{D^*} = 0$. The critical values were
299 defined as in (ISO13528 2005) and results with $|\zeta| < 2$ were considered as satisfactory, $2 \leq |\zeta| <$
300 3 as questionable and $|\zeta| \geq 3$ as unsatisfactory.

301 The ratio between the slopes of the calibration curves from samples irradiated at CINF and
302 PTB, where PTB was used as the reference, was calculated to provide a relative biological
303 effectiveness (ICRP 2003) between the two neutron fields.

304 To analyze whether laboratory-specific effects have to be considered for the estimation of
305 calibration curves or if the data from different laboratories can be pooled, quasi-Poisson
306 regression models were applied using the data from all laboratories together, comparing two
307 different models. For the first model, the data were pooled without considering a laboratory
308 effect and for the second model, the laboratory effect was included into the model by modelling
309 an interaction effect between lab and dose. The two models were compared by ANOVA F-
310 Tests, where a significant result indicates that model 2 outperforms model 1 and laboratory
311 effects should therefore be considered, i.e. there are systematic differences between dicentric
312 counts provided by the laboratories.

313 **Results**

314 *Comparison of calibration curves*

315 In the first part of the project, seven laboratories provided manually, four laboratories manually
316 and semi-automatically and one laboratory only semi-automatically scored calibration curve
317 data. Besides L8 all laboratories manually scored at least the required 1000 cells for the 0 Gy
318 data point (Table 1). As expected, the number of manually scored cells necessary to obtain 100
319 dicentrics decreased with increasing dose (Table 1). For all laboratories, the number of semi-
320 automatically captured cells was higher for samples irradiated at PTB than at CINF for each of
321 the analyzed doses (Table 1). Generally, the number of semi-automatically scored cells
322 decreased strongly with increasing dose and some laboratories were not able to capture more
323 than 500 cells for doses ≥ 2 Gy.

324 For manually scored calibration curves, the slopes (α coefficient in dicentrics per cell) ranged
325 between 0.80 and 1.13 for samples irradiated at CINF and between 0.53 and 0.78 for samples
326 irradiated at PTB (shown in Table 1 and Fig. 2a-d). The estimated slopes were significantly
327 higher (paired t-test; $P < 0.0001$, Fig. 2c) for samples from CINF than for samples from PTB and
328 the relative biological effectiveness between the two neutron fields was very similar for all
329 laboratories, ranging between 1.3 and 1.5 with a median of 1.4. Evaluation of differences
330 between laboratories revealed a strong correlation (Spearman's $\rho = 1$, $P = 0.0004$) of slopes
331 between calibration curves for samples irradiated at CINF and PTB, suggesting systematic
332 differences in the analysis of dicentric chromosomes between the laboratories (shown in Fig.
333 2d). To further test whether differences in the analysis of dicentric chromosomes between
334 laboratories should be considered, calibration curves from the pooled data of all laboratories
335 were estimated with and without including laboratory as a predictor variable in the regression
336 models. The results suggested that there is a laboratory effect, resulting in differences in the
337 slopes of the calibration curves between laboratories (ANOVA F-Test; $P < 0.0001$).

338 The slopes for the semi-automatically scored calibration curves ranged between 0.23 and 0.33
339 for samples irradiated at CINF and 0.15 and 0.25 for samples irradiated at PTB (shown in Table
340 1 and Fig. 2e-h). Again, samples irradiated at CINF showed significantly higher slopes (paired
341 t-test; $P=0.006$; Fig. 2g) compared to samples from PTB. The relative biological effectiveness
342 between the two neutron fields was relatively consistent for the participating laboratories and
343 ranged between 1.1 and 1.7 with a median of 1.3. Compared to manual scoring, the slopes from
344 semi-automatically scored samples were on average consistently 70% lower. Consideration of
345 differences between laboratories showed two clusters (shown in Fig. 2e-h and Table 1) of semi-
346 automatically scored calibration curves for samples irradiated at CINF as well as for PTB with
347 low slopes (L2 and L6) and higher slopes (L1, L4 and L7). In contrast to manual scoring, the
348 correlation of slopes between calibration curves from samples irradiated at CINF and PTB was
349 not significant (Spearman's $\rho=0.5$, $P=0.45$; Fig. 2h). However, regression models including
350 laboratory as a predictor variable again suggested that there is a laboratory effect (ANOVA F-
351 Test; $P<0.0001$). The latter observation can very likely be attributed to the clustering of slopes
352 between laboratories.

353 Most of the manually scored results from doses ≤ 1 Gy showed a tendency for overdispersion
354 ($\delta > 1$) with many reaching significance (Supplementary Figure 1a-d). In contrast, for doses >1
355 Gy, the dispersion levels decreased and at the highest dose, a tendency for underdispersion was
356 often observed (Supplementary Figure 1a-d). Semi-automatically scored samples showed
357 significant overdispersion for all doses >0 Gy and the dispersion levels increased with dose or
358 were approximately constant (Supplementary Figure 1e-h).

359

360 *Dose estimates for test samples*

361 After the establishment of calibration curves, dose estimates for test samples with blinded doses
362 were performed to validate the applicability of the calibration curves and to test the performance
363 of the participating laboratories. Each neutron facility provided three irradiated test samples
364 (Blind 2-4) and included one sham-irradiated sample (Blind 1). The dose estimates were
365 obtained using the laboratory specific calibration curves established at the same irradiation
366 facility as the test samples. The number of scored metaphases (in full mode) for the test samples
367 can be found in Table 2.

368 For manually scored dicentric chromosomes, a good agreement between biological dose
369 estimates and the physical reference doses was observed for samples from both irradiation
370 facilities for triage as well as for full scoring mode (shown in Fig. 3 and Table 3). For samples
371 irradiated at CINF, all of the estimated doses included the reference dose in the 95% CI, all or
372 almost all were within ± 0.5 Gy or ± 0.25 Gy of the reference dose (shown in Fig. 3 and Table
373 3) and all estimates showed $|\zeta| < 2$ (shown in Fig. 4 and Table 3). Details on the definition of ζ -
374 scores can be found in Materials and Methods. For samples irradiated at PTB, dose estimates
375 showed an increased deviation from reference doses in comparison to samples irradiated at
376 CINF (shown in Fig. 3 and Table 3). Here, at least 50% (full) or 67% (triage) estimated doses
377 included the reference dose in the 95% CI, were within ± 0.25 Gy or within ± 0.5 Gy of the
378 reference dose (shown in Fig. 3 and Table 3) and showed $|\zeta| < 2$ (shown in Fig. 4 and Table 3).
379 The control sample was detected by all participants for samples from CINF as well as from
380 PTB.

381 For semi-automatically scored dicentric chromosomes, the agreement between the biological
382 dose estimates and the physical reference doses was worse compared to manual scoring with
383 regard to ζ -scores ($|\zeta| < 2$). Moreover, fewer dose estimates included the physical reference dose
384 in the estimated 95% CI and fewer dose estimates were within ± 0.25 Gy or ± 0.5 Gy of the

385 reference dose (shown in Fig. 3 & 4 and Table 3). Moreover, manually scored results of the
386 irradiated test samples consistently showed lower variability in terms of the coefficient of
387 variation (Table 3; CINF: CV between 0.07 and 0.12; PTB: CV between 0.14 and 0.17) than
388 semi-automatically scored results (CINF: CV between 0.21 and 0.28; PTB: CV between 0.26
389 and 0.42).

390 Test samples that were manually scored in full mode generally showed a tendency for
391 overdispersion ($\delta > 1$) for doses < 1 Gy for both irradiation facilities (Table 3 and Supplementary
392 Figure 2). The percentage of results with significant overdispersion decreased with increasing
393 dose (Table 3). For semi-automatic scoring in full mode, all test samples with doses > 0 Gy
394 showed overdispersion, independent of dose and irradiation facility (Supplementary Figure 2
395 and Table 3). Correspondingly, significant overdispersion ($P < 0.05$) was observed for 100%
396 (CINF) and for 87% (PTB) of the irradiated (> 0 Gy) test samples.

397

398 **Discussion**

399 In the case of a large-scale radiological or nuclear event, biological dosimetry can be an
400 important tool to aid clinical decision-making and to identify non-exposed “worried-well”
401 individuals. Networking between international laboratories is one approach to handle the large
402 sample size to be analyzed during such an event. To enable reliable dose estimation or
403 categorizations of individuals into clinically relevant groups, the laboratories for biological
404 dosimetry must establish calibration curves from different radiation qualities. While most
405 RENEB laboratories have well established calibration curves based on the DCA for low-LET
406 γ -rays or X-rays which have been validated in several exercises (Endesfelder et al. 2021;
407 Gregoire et al. 2021; Oestreicher et al. 2017), the situation is different for exposures with
408 neutrons, where the number of laboratories with validated calibration curves is certainly lower.
409 Moreover, the distribution of the energy spectrum of the neutrons has a significant influence on
410 the biological effectiveness (ICRP 2003; Pandita and Geard 1996; Schmid et al. 2003; Tanaka
411 et al. 1999), and it might therefore not be sufficient to have a single neutron calibration curve
412 per laboratory. In the frame of the BALANCE project, an exposure similar to a Hiroshima-like
413 device at a distance of 1.5 km from the epicenter was simulated. At this distance the neutrons
414 have a broad energy spectrum, spanning energies from thermal up to about 10 MeV (Egbert et
415 al. 2007), and the field is composed of a mixture of neutrons and photons. To enable the
416 comparison of differences in the biological effectiveness between the two neutron sources
417 resulting from differences in the shape of the applied energy spectra, blood samples were
418 irradiated at two different facilities in Germany (PTB) and USA (CINF). The practicability of
419 the shipment of blood samples between Germany and USA was tested by sending samples in
420 both directions. In a first step calibration curves for the DCA were established by each
421 participating RENEB laboratory and the differences in the biological effectiveness were
422 evaluated between the two irradiation facilities. Next, to test the applicability of the calibration
423 curves and to validate the performance of the participating RENEB laboratories four test

424 samples with blinded doses were irradiated at each PTB and CINF and sent to the participants
425 for dose estimation. To test the validity of the DCA for neutron exposures greater than 1 Gy,
426 blood samples were exposed to doses ranging from 0 Gy to 4 Gy.

427

428 The neutron spectra from both irradiation facilities approximately cover the range of the energy
429 spectrum from the Hiroshima bomb at a distance of 1.5 km from the epicenter. Nevertheless,
430 the calibration curves obtained by the participating laboratories from the RENE network
431 strongly suggested that the biological effectiveness of irradiations at CINF is in median 1.4
432 times higher compared to irradiations at PTB. This result was consistently observed by all
433 participating laboratories, which strongly suggested a systematic difference that was not
434 expected to this extent when the project started. A closer inspection of the neutron energy
435 spectra revealed differences in the shape of the energy distributions. While the contribution of
436 energies <0.7 MeV and >3 MeV is higher for CINF, the contribution of energies in the range
437 of 1-3 MeV is higher for PTB. The tissue-kerma weighted mean energy of the PTB neutron
438 field was about 2.5 MeV and the one at CINF was about 3.2 MeV. From the literature on
439 monoenergetic neutrons, it can be expected, that the relative biological effectiveness compared
440 to γ -rays should be increased if the contributions of energies in the range of approximately 0.2-
441 0.5 MeV is higher compared to energies >1 MeV (Pandita and Geard 1996; Schmid et al. 2003;
442 Tanaka et al. 1999). Hence, it is likely that the observed differences in the biological
443 effectiveness can be caused by differences in the distribution of the energy spectra of the two
444 irradiation facilities. However, to exactly quantify the expected difference further research will
445 be required in future. Although it can be assumed that donor effects and differences in transport
446 times did not significantly influence the results, it should be noted that blood samples from
447 different donors were used at PTB and CINF to simulate real accident scenarios and that the
448 transport time from the irradiation facilities to BfS differed slightly, but within an acceptable
449 range. Sending blood samples between EU and non-EU countries is always a challenge. In the

450 BALANCE project, the transportation between USA and Germany was successfully completed
451 within 48 h underlining the need to use specialized express services for diagnostic material to
452 avoid any delays. For optimal shipment conditions the use of temperature-controlled
453 thermoboxes can be recommended to prevent extreme temperatures which make the stimulation
454 of lymphocytes more difficult.

455

456 The calibration curves of the participants showed a significant laboratory effect. The differences
457 between the slopes of the manually scored calibration curves were highly correlated between
458 samples irradiated at CINF and PTB, i.e. the laboratories that scored higher or lower numbers
459 of dicentric chromosomes for samples irradiated at CINF scored also higher or lower numbers
460 of dicentric chromosomes for samples irradiated at PTB. The latter strongly suggested a
461 systematic laboratory effect, which is probably related to different scoring criteria. For semi-
462 automatically scored calibration curves, two clusters of laboratories were observed, consistently
463 having either lower or higher numbers of dicentric chromosomes, which again suggested a
464 systematic difference between these laboratories. This might be related to the use of different
465 classifiers for the automatic detection of dicentric chromosomes.

466

467 The current recommendation for biological dosimetry for the exposure to high-LET radiation
468 is to establish calibration curves for the DCA in the dose range 0 Gy to 2 Gy (IAEA 2011) and
469 there is currently little research on the DCA for neutron doses greater than 2 Gy. One of the
470 aims of this project was therefore, to establish calibration curves including higher doses of up
471 to 4 Gy. Such high neutron doses will in most cases be lethal but might be relevant for biological
472 dosimetry in the case of inhomogeneous or partial body exposures. For this purpose, each
473 participating laboratory from the RENEB network used the calibration curves established in the
474 first part of the BALANCE project to provide dose estimates for the test samples. While the
475 manually scored results showed a good agreement with the physical reference doses in the

476 whole dose range tested, especially for samples irradiated at CINF, the semi-automatically
477 scored results revealed some problems. As a consequence, semi-automatic scoring for high-
478 LET neutron exposures should be further validated and only be used if the validity of the
479 approach was ensured. The good performance of most RENE B laboratories for dose estimates
480 obtained based on manual scoring suggested that RENE B laboratories were able to successfully
481 estimate neutron doses based on the pre-established calibration curves irradiated at the same
482 source and conditions as the test samples. However, it should be noted that the exact neutron
483 energy spectrum will in most cases not be known in a real-life scenario and could also vary
484 based on the location. Calibration curves that exactly mimic the exposure situation might not
485 be available to the laboratories performing biological dosimetry. Nevertheless, within the frame
486 of the BALANCE project, all RENE B participants established new calibration curves for
487 neutron exposures based on two different neutron spectra approximately simulating the
488 spectrum of the Hiroshima bombing at a distance of 1.5 km from the epicenter, which can be
489 further validated and potentially be used in real-life exposure scenarios in the future.

490

491 The distribution of dicentric chromosomes after high-LET neutron irradiation is generally
492 known to show overdispersion (Heimers et al. 2005; Schmid et al. 2000; Schmid 1998), i.e. the
493 variance is larger than the mean and the data is therefore not Poisson distributed as for acute
494 whole-body low-LET exposures. However, most studies focusing on dicentric chromosomes
495 for high-LET neutron exposures analyzed doses ≤ 1 Gy. In concordance with data shown
496 elsewhere (Heimers et al. 2005; Schmid et al. 2000; Schmid 1998), most of the manually scored
497 results from doses ≤ 1 Gy showed overdispersion ($\delta > 1$). In contrast, for doses > 1 Gy,
498 considerably fewer of the manually scored results showed overdispersion and dispersion levels
499 seemed to decrease with increasing dose for doses > 1 Gy. This observation might indicate that
500 the exposure is more uniform for higher doses, i.e. each cell has the same probability to develop
501 dicentric chromosomes. Another explanation is that the variance decreases relative to the mean

502 due to saturation effects. The observation that the dispersion levels are not constant with doses
503 complicates an adequate consideration of dispersion for the estimation of the uncertainties, as
504 most models (e.g. quasi-Poisson regression models) assume constant overdispersion. In
505 contrast, all semi-automatically scored samples showed overdispersion over the whole dose
506 range >0 Gy and 95% of the samples showed significant overdispersion. While a decreasing
507 trend of dispersion levels with increasing dose was observed for manual scoring, the dispersion
508 levels rather increased or were approximately constant for the semi-automatically scored data.
509 This observation is in concordance with published data, where overdispersion was reported for
510 semi-automatic scoring due to differences in the number of detected chromosomes related to
511 variable quality of the metaphases (Endesfelder et al. 2020). The differences in the dispersion
512 patterns between manual and semi-automatic scoring strongly suggest that different methods
513 for the assessment of uncertainties should be applied.

514 **Conclusions**

515 The research presented in this publication provides new insights into the applicability of
516 cytogenetic biomarkers for dose estimations in the case of a neutron exposure with a spectrum
517 similar to the Hiroshima bombing. Critical points, such as high doses and neutron energy
518 spectra, practicability of the shipment of blood samples and the applicability of calibration
519 curves for different emergency situations were tested and evaluated in a transatlantic
520 cooperation of laboratories from Europe and the US. Interestingly, differences in the biological
521 effectiveness of different neutron irradiation facilities could be revealed. While the manually
522 scored results suggested that RENEB laboratories were able to successfully resolve the doses,
523 the results based on semi-automatically scored data were more biased, suggesting that further
524 research is needed.

525

526 **Statement of Ethics**

527 In Germany, blood samples from healthy adult donors were obtained by physicians according
528 to §15 of the code of medical ethics for physicians in Bavaria, Germany, following the
529 principles of the Declaration of Helsinki. In the US blood was collected under Columbia
530 University IRB protocol AAAS3035.

531

532 **Conflict of Interest Statement**

533 The authors have no conflicts of interest to declare.

534

535 **Funding Sources**

536 This work was supported by grant number U19-AI067773 to the Center for High-Throughput
537 Minimally Invasive Radiation Biodosimetry, from the National Institute of Allergy and
538 Infectious Diseases (NIAID), National Institutes of Health (NIH). The content is solely the
539 responsibility of the authors and does not necessarily represent the official views of the NIAID
540 or NIH.

541 **Acknowledgement**

542 The authors thank the operators and technical staff of the PTB and CINF accelerator facilities
543 and of the participating RENEB partners.

544

545 **Author contributions**

546 UK, UO, UG, GG, AW organized and conducted the irradiations and distribution of blood
547 samples. UO, MB, CB, MP, GG, EG, GT, ST, EA, LM, MS, MJP, MMD, JFB, MP-C, AV, AB
548 provided dose estimates based on the DCA. DE did the statistical evaluation of the ILC results
549 and wrote the manuscript. All authors reviewed and revised the manuscript.

550 Conflict of Interest Statement

551

552 **Data availability statement**

553 All data generated or analyzed during this study are included in this article. Further enquiries
554 can be directed to the corresponding author.

555

556 **Figure Legends**

557 **Figure 1: Irradiation of samples and comparison of neutron fields for the two irradiation**
558 **facilities. a&b:** Position and mounting of the samples at PTB (a) and CINF (b). **C:** Calculated
559 tissue-kerma-weighted relative energy distributions of the neutron fields (neutron fluence *
560 kerma factors k_{ϕ}), PTB (blue), CINF (red) and for the Hiroshima bombing at approximately 1.5
561 km from the epicenter (black).

562 **Figure 2: Calibration curves from RENEb participants for irradiations at PTB and CINF**
563 **and comparison of slopes. a&b:** Linear calibration curves from manual scoring for irradiations
564 performed at PTB (a) and CINF (b). **c:** Boxplots comparing the slopes of manually scored
565 calibration curves from irradiations performed at PTB and CINF. **d:** Correlation of slopes of
566 manually scored calibration curves between irradiations performed at PTB and CINF. **e&f:**
567 Linear calibration curves from semi-automatic scoring for irradiations performed at PTB (e)
568 and CINF (f). Different line colors and symbols indicate the participating laboratories from the
569 RENEb network. **g:** Boxplots comparing the slopes of semi-automatically scored calibration
570 curves from irradiations performed at PTB and CINF. **h:** Correlation of slopes of semi-
571 automatically scored calibration curves between irradiations performed at PTB and CINF.

572 **Figure 3: DCA-based dose estimates for test samples provided by the participating**
573 **RENEb laboratories.** Each plot shows the dose estimates and the corresponding 95%
574 confidence intervals (error bars) provided by the eight participating RENEb laboratories (x-
575 axis). The results for manual scoring are shown in black (triage mode scoring) and blue (full
576 mode scoring) and the results for semi-automatic scoring in orange (triage mode scoring) and
577 red (full mode scoring). The asterisks indicate dose estimates where the corresponding 95%
578 confidence intervals did not include the physical reference dose. Data from replicate slides was
579 pooled for each test sample.

580 **Figure 4: Comparison of DCA-based dose estimates with physical reference doses. a&b:**
581 Difference between DCA-based dose estimates and physical reference doses (y-axis) for the
582 eight participating RENEb laboratories (x-axis) from test samples irradiated with doses >0 Gy
583 at PTB (**a**) and CINF (**b**). The horizontal lines show the intervals of ± 0.25 Gy (cyan) or ± 0.5
584 Gy (blue) around the physical reference dose. **c&d:** ζ -score (y-axis) for the eight participating
585 RENEb laboratories (x-axis) from test samples irradiated with doses >0 Gy at PTB (**c**) and
586 CINF (**d**). The horizontal lines indicate ζ -scores of ± 2 (cyan) or ± 3 (blue), respectively. Results
587 with $|\zeta| < 2$ are considered as satisfactory, $2 \leq |\zeta| < 3$ as questionable and $|\zeta| \geq 3$ as unsatisfactory.
588 The results for manual scoring are shown in gray (triage mode scoring) and black (full mode
589 scoring) and the results for semi-automatic scoring in orange (triage mode scoring) and red (full
590 mode scoring). Some laboratories performed only manual (L3, L5, L8) and some only semi-
591 automatic scoring (L6 for samples irradiated at CINF and L7) and one lab (L6) performed the
592 manual scoring only in full mode for samples irradiated at PTB.

593 **References**

594

595 Beinke C, Ben-Shlomo A, Abend M, Port M: A Case Report: Cytogenetic Dosimetry after Accidental
596 Radiation Exposure during ¹⁹²Ir Industrial Radiography Testing. *Radiation Research* 184:66-72 (2015).
597 Bloom A, Neriishi S, Kamada N, Iseki T, Keehn R: Cytogenetic Investigation of Survivors of the Atomic
598 Bombings of Hiroshima and Nagasaki. *The Lancet* 288:672-674 (1966).
599 Brede HJ, Cosack M, Dietze G, Gumpert H, Guldbakke S, Jahr R, Kutscha M, Schlegel-Bickmann D,
600 Schölermann H: The Braunschweig accelerator facility for fast neutron research. *Nuclear Instruments*
601 *and Methods* 169:349-358 (1980).
602 Broustas CG, Harken AD, Garty G, Amundson SA: Identification of differentially expressed genes and
603 pathways in mice exposed to mixed field neutron/photon radiation. *BMC Genomics* 19:504 (2018).
604 Buddemeier B, Dillon M: Key Response Planning Factors for the Aftermath of Nuclear Terrorism.
605 *Environmental Science* (2009).
606 Dobson RL, Straume T, Carrano AV, Minkler JL, Deaven LL, Littlefield LG, Awa AA: Biological
607 effectiveness of neutrons from Hiroshima bomb replica: results of a collaborative cytogenetic study.
608 *Radiat Res* 128:143-149 (1991).
609 Egbert SD, Kerr GD, Cullings HM: DS02 fluence spectra for neutrons and gamma rays at Hiroshima
610 and Nagasaki with fluence-to-kerma coefficients and transmission factors for sample measurements.
611 *Radiat Environ Biophys* 46:311-325 (2007).
612 Endesfelder D, Kulka U, Einbeck J, Oestreicher U: Improving the accuracy of dose estimates from
613 automatically scored dicentric chromosomes by accounting for chromosome number. *Int J Radiat*
614 *Biol* 96:1571-1584 (2020).
615 Endesfelder D, Oestreicher U, Kulka U, Ainsbury EA, Moquet J, Barnard S, Gregoire E, Martinez JS,
616 Trompier F, Ristic Y, Woda C, Waldner L, Beinke C, Vral A, Barquinero JF, Hernandez A, Sommer S,
617 Lumniczky K, Hargitai R, Montoro A, Milic M, Monteiro Gil O, Valente M, Bobyk L, Sevriukova O,
618 Sabatier L, Prieto MJ, Moreno Domene M, Testa A, Patrono C, Terzoudi G, Triantopoulou S, Histova R,
619 Wojcik A: RENE/ EURADOS field exercise 2019: robust dose estimation under outdoor conditions
620 based on the dicentric chromosome assay. *Int J Radiat Biol* 97:1181-1198 (2021).
621 Fajgelj A, Horvat D, Pucelj B: Chromosome aberrations induced in human lymphocytes by U-235
622 fission neutrons. Part II: Evaluation of the effect of the induced Na-24 activity on the chromosomal
623 aberration yield. *Strahlenther Onkol* 168:406-411 (1992).
624 Garty G, Chen Y, Salerno A, Turner H, Zhang J, Lyulko O, Bertucci A, Xu Y, Wang H, Simaan N, Randers-
625 Pehrson G, Yao YL, Amundson SA, Brenner DJ: The Rabbit: A Rapid Automated Biodosimetry Tool for
626 Radiological Triage. *Health physics* 98:209-217 (2010).
627 Garty G, Xu Y, Elliston C, Marino SA, Randers-Pehrson G, Brenner DJ: Mice and the A-Bomb:
628 Irradiation Systems for Realistic Exposure Scenarios. *Radiation Research* 187:475-485 (2017).
629 Gregoire E, Barquinero JF, Gruel G, Benadjaoud M, Martinez JS, Beinke C, Balajee A, Beukes P, Blakely
630 WF, Dominguez I, Duy PN, Gil OM, Güçlü I, Guogyte K, Hadjidekova SP, Hadjidekova V, Hande P, Jang
631 S, Lumniczky K, Meschini R, Milic M, Montoro A, Moquet J, Moreno M, Norton FN, Oestreicher U,
632 Pajic J, Sabatier L, Sommer S, Testa A, Terzoudi G, Valente M, Venkatachalam P, Vral A, Wilkins RC,
633 Wojcik A, Zafiroopoulos D, Kulka U: RENE Inter-Laboratory comparison 2017: limits and pitfalls of
634 ILCs. *International Journal of Radiation Biology* 97:888-905 (2021).
635 Güçlü I: Cytogenetic follow-up of an individual after accidental exposure to industrial radiation using
636 dicentric frequency in blood lymphocytes. *Mutation research* 861-862:503276 (2021).
637 Heimers A, Brede HJ, Giesen U, Hoffmann W: Influence of mitotic delay on the results of biological
638 dosimetry for high doses of ionizing radiation. *Radiat Environ Biophys* 44:211-218 (2005).
639 Heimers A, Brede HJ, Giesen U, Hoffmann W: Chromosome aberration analysis and the influence of
640 mitotic delay after simulated partial-body exposure with high doses of sparsely and densely ionising
641 radiation. *Radiat Environ Biophys* 45:45-54 (2006).
642 IAEA: Cytogenetic Dosimetry: Applications in Preparedness for and Response to Radiation
643 Emergencies. EPR-Biodosimetry, International Atomic Energy Agency, Vienna (2011).

644 ICRP: Relative Biological Effectiveness (RBE), Quality Factor (Q), and Radiation Weighting Factor (wR).
645 ICRP Publication 92 Ann. ICRP 33 (4) (2003).
646 ICRU: ICRU Report No.45, Clinical neutron dosimetry, part I: determination of absorbed dose in a
647 patient treated by external beams of fast neutrons. ICRU, International Commission on Radiation
648 Units and Measurements, Bethesda, Maryland (1989).
649 ISO13528: Statistical methods for use in proficiency testing by interlaboratory comparisons. Geneva
650 (2005).
651 ISO19238: International Organization for Standardization (ISO) , Radiation protection performance
652 criteria for service laboratories performing biological dosimetry by cytogenetics. Geneva ISO
653 19238:2014 (2014).
654 Kramer K, Li A, Madrigal J, Sanchez B, Millage K: Monte Carlo Modeling of the Initial Radiation
655 Emitted by an Improvised Nuclear Device in the National Capital Region (Revision 1), (2016).
656 Kulka U, Abend M, Ainsbury EA, Badie C, Barquinero JF, Barrios L, Beinke C, Bortolin E, Cucu A, De
657 Amicis A, Domínguez I, Fattibene P, Frøvig AM, Gregoire E, Guogyte K, Hadjidekova V, Jaworska A,
658 Kriehuber R, Lindholm C, Lloyd D, Lumniczky K, Lyng F, Meschini R, Mörtl S, Della Monaca S, Monteiro
659 Gil O, Montoro A, Moquet J, Moreno M, Oestreicher U, Palitti F, Pantelias G, Patrono C, Piqueret-
660 Stephan L, Port M, Prieto MJ, Quintens R, Ricoul M, Romm H, Roy L, Sáfrány G, Sabatier L, Sebastia N,
661 Sommer S, Terzoudi G, Testa A, Thierens H, Turai I, Trompier F, Valente M, Vaz P, Voisin P, Vral A,
662 Woda C, Zafiroopoulos D, Wojcik A: RENEb – Running the European Network of biological dosimetry
663 and physical retrospective dosimetry. *International Journal of Radiation Biology* 93:2-14 (2016).
664 Kulka U, Wojcik A, Di Giorgio M, Wilkins R, Suto Y, Jang S, Quing-Jie L, Jiaxiang L, Ainsbury EA, Woda
665 C, Roy L, Li C, Lloyd D, Carr Z: Biodosimetry and Biodosimetry Networks for Managing Radiation
666 Emergency. *Radiation Protection Dosimetry* 182:128-138 (2018).
667 Laiakis E, Canadell M, Grilj V, Harken A, Garty G, Astarita G, Brenner D, Smilenov L, Fornace A: Serum
668 lipidomic analysis from mixed neutron/X-ray radiation fields reveals a hyperlipidemic and pro-
669 inflammatory phenotype. *Sci Rep* 9:4539 (2019).
670 Laiakis EC, Wang YW, Young EF, Harken AD, Xu Y, Smilenov L, Garty GY, Brenner DJ, Fornace AJ, Jr.:
671 Metabolic Dysregulation after Neutron Exposures Expected from an Improvised Nuclear Device.
672 *Radiat Res* 188:21-34 (2017).
673 Malmer CJ: ICRU Report 63. Nuclear Data for Neutron and Proton Radiotherapy and for Radiation
674 Protection. *Medical Physics* 28:861-861 (2001).
675 Meadows JW: The $^9\text{Be}(d, n)$ thick-target neutron spectra for deuteron energies between 2.6 and 7.0
676 MeV. *Nuclear Instruments and Methods in Physics Research Section A: Accelerators, Spectrometers,*
677 *Detectors and Associated Equipment* 324:239-246 (1993).
678 Mukherjee S, Grilj V, Broustas CG, Ghandhi SA, Harken AD, Garty G, Amundson SA: Human
679 Transcriptomic Response to Mixed Neutron-Photon Exposures Relevant to an Improvised Nuclear
680 Device. *Radiat Res* 192:189-199 (2019).
681 Oestreicher U, Endesfelder D, Gomolka M, Kesminiene A, Lang P, Lindholm C, Rossler U, Samaga D,
682 Kulka U: Automated scoring of dicentric chromosomes differentiates increased radiation sensitivity
683 of young children after low dose CT exposure in vitro. *Int J Radiat Biol* 94:1017-1026 (2018).
684 Oestreicher U, Samaga D, Ainsbury EA, Antunes AC, Baeyens A, Barrios L, Beinke C, Beukes P, Blakely
685 WF, Cucu A, De Amicis A, Depuydt J, De Sanctis S, Di Giorgio M, Dobos K, Dominguez I, Duy PN,
686 Espinoza ME, Flegal FN, Figel M, Garcia O, Monteiro Gil O, Gregoire E, Guerrero-Carbajal C, Guclu I,
687 Hadjidekova V, Hande P, Kulka U, Lemon J, Lindholm C, Lista F, Lumniczky K, Martinez-Lopez W,
688 Maznyk N, Meschini R, M'Kacher R, Montoro A, Moquet J, Moreno M, Noditi M, Pajic J, Radl A, Ricoul
689 M, Romm H, Roy L, Sabatier L, Sebastia N, Slabbert J, Sommer S, Stuck Oliveira M, Subramanian U,
690 Suto Y, Que T, Testa A, Terzoudi G, Vral A, Wilkins R, Yanti L, Zafiroopoulos D, Wojcik A: RENEb
691 intercomparisons applying the conventional Dicentric Chromosome Assay (DCA). *Int J Radiat Biol*
692 93:20-29 (2017).
693 Pandita TK, Geard CR: Chromosome aberrations in human fibroblasts induced by monoenergetic
694 neutrons. I. Relative biological effectiveness. *Radiat Res* 145:730-739 (1996).

695 Repin M, Pampou S, Karan C, Brenner DJ, Garty G: RABiT-II: Implementation of a High-Throughput
696 Micronucleus Biodosimetry Assay on Commercial Biotech Robotic Systems. *Radiat Res* 187:502-508
697 (2017).

698 Romm H, Ainsbury EA, Barnard S, Barrios L, Barquinero JF, Beinke C, Deperas M, Gregoire E,
699 Koivistoinen A, Lindholm C, Moquet J, Oestreicher U, Puig R, Rothkamm K, Sommer S, Thierens H,
700 Vandersickel V, Vral A, Wojcik A: Automatic scoring of dicentric chromosomes as a tool in large scale
701 radiation accidents. *Mutation research* 756:174-183 (2013).

702 Rossi HH, Bateman JL, Bond VP, Goodman LJ, Stickley EE: The dependence of RBE on the energy of
703 fast neutrons: 1. Physical design and measurement of absorbed dose. *Radiat Res* 13:503-520 (1960).

704 Royba E, Repin M, Pampou S, Karan C, Brenner DJ, Garty G: RABiT-II-DCA: A Fully-automated
705 Dicentric Chromosome Assay in Multiwell Plates. *Radiat Res* 192:311-323 (2019).

706 Salassidis K, Schmid E, Peter RU, Braselmann H, Bauchinger M: Dicentric and translocation analysis
707 for retrospective dose estimation in humans exposed to ionising radiation during the Chernobyl
708 nuclear power plant accident. *Mutation Research/Fundamental and Molecular Mechanisms of*
709 *Mutagenesis* 311:39-48 (1994).

710 Sasaki MS, Endo S, Ejima Y, Saito I, Okamura K, Oka Y, Hoshi M: Effective dose of A-bomb radiation in
711 Hiroshima and Nagasaki as assessed by chromosomal effectiveness of spectrum energy photons and
712 neutrons. *Radiat Environ Biophys* 45:79-91 (2006).

713 Savage JRK, Papworth DG: Constructing a 2B Calibration Curve for Retrospective Dose
714 Reconstruction. *Radiation Protection Dosimetry* 88:69-76 (2000).

715 Schmid E, Regulla D, Guldbakke S, Schlegel D, Bauchinger M: The effectiveness of monoenergetic
716 neutrons at 565 keV in producing dicentric chromosomes in human lymphocytes at low doses. *Radiat*
717 *Res* 154:307-312 (2000).

718 Schmid E, Schlegel D, Guldbakke S, Kapsch RP, Regulla D: RBE of nearly monoenergetic neutrons at
719 energies of 36 keV-14.6 MeV for induction of dicentrics in human lymphocytes. *Radiation and*
720 *Environmental Biophysics* 42:87-94 (2003).

721 Schmid E, Wagner FM, Romm H, Walsh L, Roos H: Dose-response relationship of dicentric
722 chromosomes in human lymphocytes obtained for the fission neutron therapy facility MEDAPP at the
723 research reactor FRM II. *Radiation and Environmental Biophysics* 48:67-75 (2008).

724 Schmid HS, M. Bauchinger, E.: Chromosome aberration frequencies in human lymphocytes irradiated
725 in a phantom by a mixed beam of fission neutrons and gamma -rays. *International Journal of*
726 *Radiation Biology* 73:263-267 (1998).

727 Tanaka K, Gajendiran N, Endo S, Komatsu K, Hoshi M, Kamada N: Neutron Energy-Dependent Initial
728 DNA Damage and Chromosomal Exchange. *Journal of Radiation Research* 40:36-44 (1999).

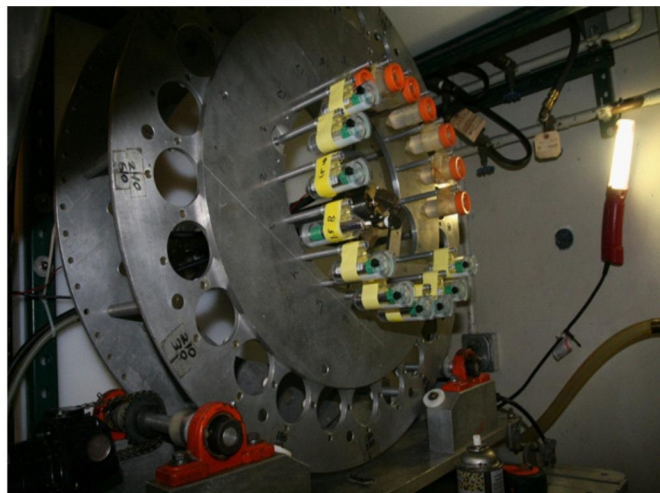
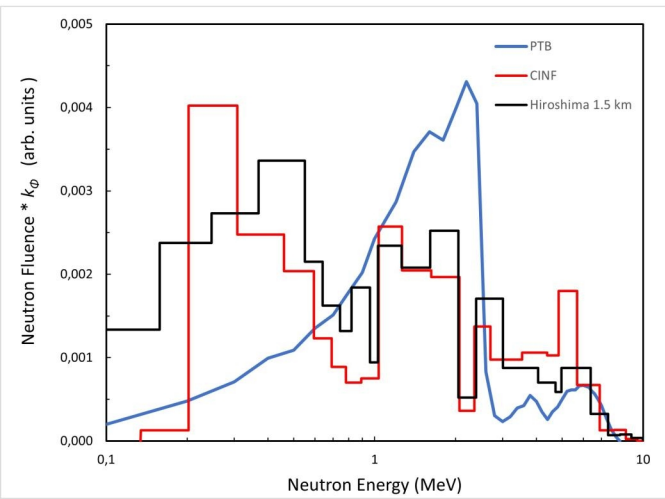
729 Tawn EJ, Curwen GB, Riddell AE: Chromosome aberrations in workers occupationally exposed to
730 tritium. *J Radiol Prot* 38:N9-N16 (2018).

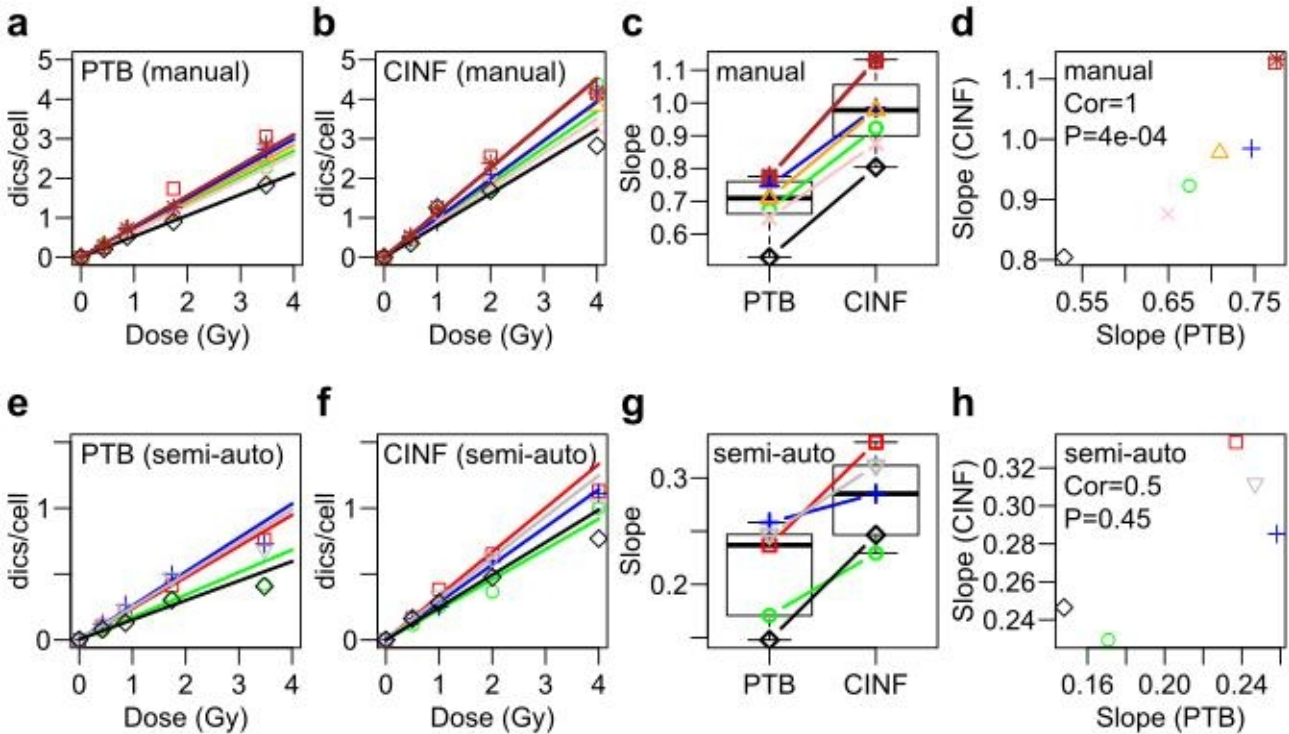
731 Wernli C, Eikenberg J, Marzocchi O, Breustedt B, Oestreicher U, Romm H, Gregoratto D, Marsh J: 30-y
732 follow-up of a Pu/Am inhalation case. *Radiat Prot Dosimetry* 164:57-64 (2015).

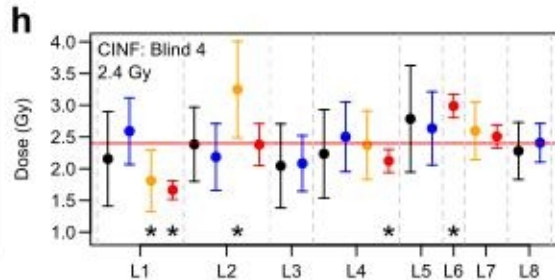
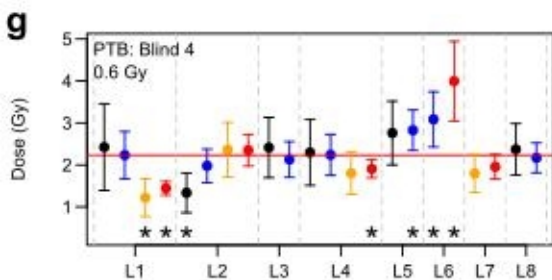
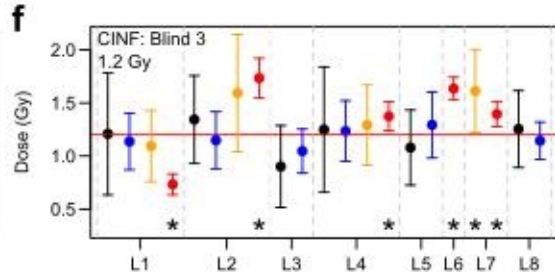
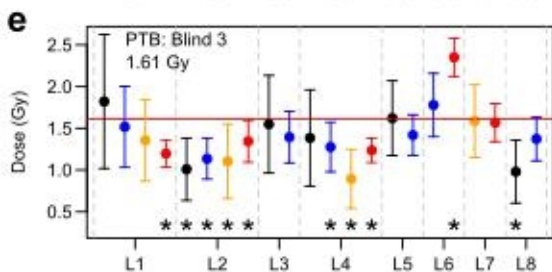
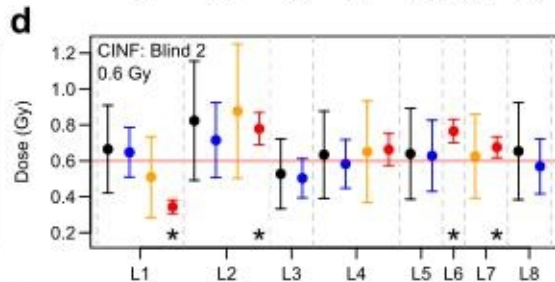
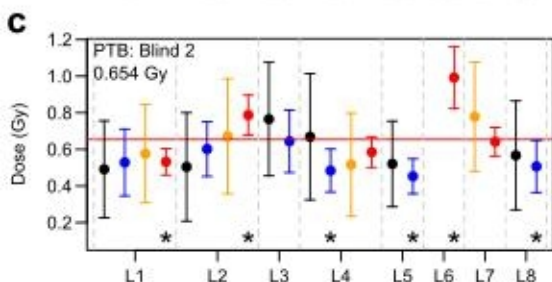
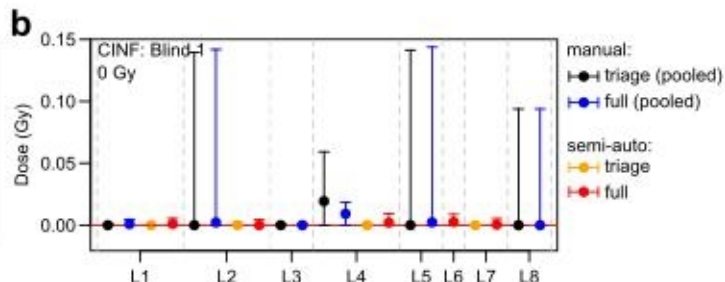
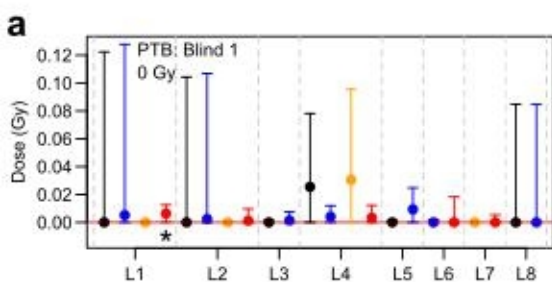
733 Xu Y, Randers-Pehrson G, Marino SA, Garty G, Harken A, Brenner DJ: Broad Energy Range Neutron
734 Spectroscopy using a Liquid Scintillator and a Proportional Counter: Application to a Neutron
735 Spectrum Similar to that from an Improvised Nuclear Device. *Nucl Instrum Methods Phys Res A*
736 794:234-239 (2015a).

737 Xu Y, Randers-Pehrson G, Turner HC, Marino SA, Geard CR, Brenner DJ, Garty G: Accelerator-Based
738 Biological Irradiation Facility Simulating Neutron Exposure from an Improvised Nuclear Device.
739 *Radiation Research* 184:404-410 (2015b).

740

a**b****c**





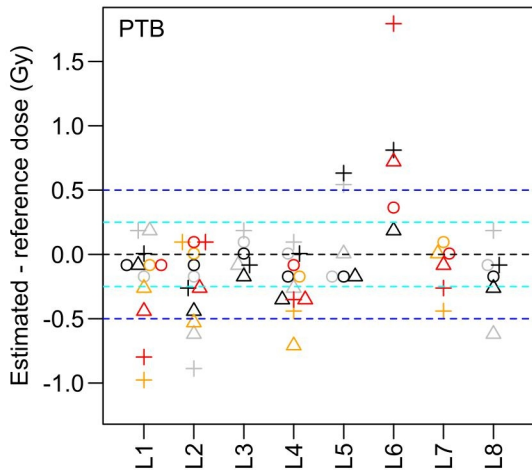
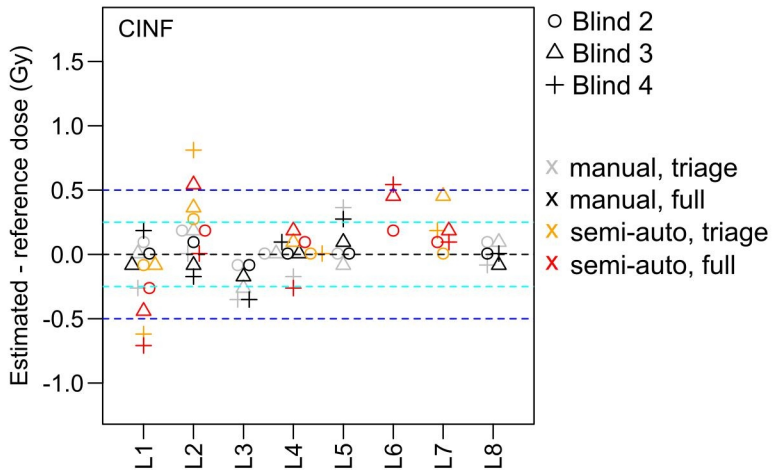
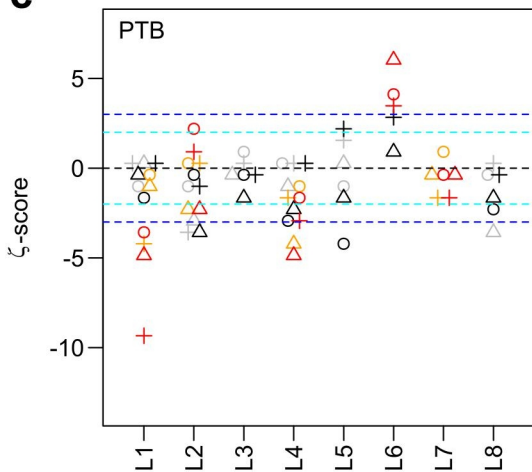
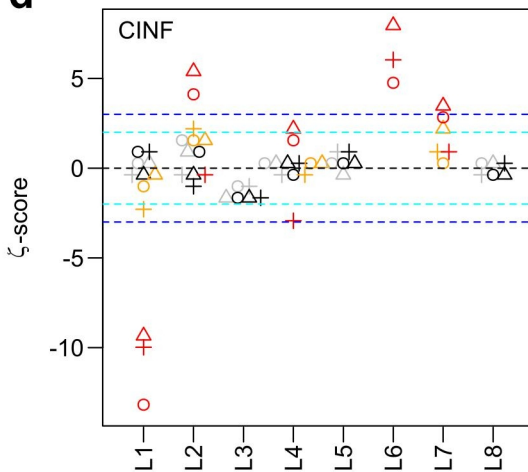
a**b****c****d**

Table 1: Number of manually and semi-automatically scored metaphases per dose and calibration curve coefficients for calibration samples irradiated at CINF and PTB. The number of scored metaphases and the number of dicentric chromosomes (in brackets) are shown for each dose point and each participating laboratory. The intercept (C) and slope (α) of the linear calibration curves and their corresponding standard errors (SE) are shown for each participating laboratory.

Facility: CINF (manual scoring)									
Lab	0 Gy	0.5 Gy	1 Gy	2 Gy	4 Gy	C	α	SE(C)	SE(α)
L1	1009 (1)	245 (118)	96 (101)	125 (318)	25 (104)	0.0010	1.1268	0.0010	0.0463
L2	1000 (0)	220 (100)	110 (102)	104 (175)	26 (114)	9.8×10^{-8}	0.9229	0.0657	0.0698
L3	1025 (1)	263 (118)	100 (107)	49 (100)	30 (115)	0.0010	0.9778	0.0010	0.0467
L4	1000 (1)	204 (100)	113 (100)	49 (102)	24 (101)	0.0010	0.9845	0.0010	0.0501
L5	1000 (0)	245 (102)	116 (108)	55 (104)	37 (121)	6.4×10^{-6}	0.8762	0.0632	0.0710
L6	1002 (4)	283 (101)	77 (97)	80 (135)	67 (189)	0.0040	0.8042	0.0028	0.0499
L8	150 (0)	346 (185)	195 (247)	199 (473)	100 (415)	1.1×10^{-5}	1.1321	0.0542	0.0501
Facility: CINF (semi-automatic scoring)									
L1	11803 (10)	6002 (994)	4548 (1740)	2868 (1865)	759 (858)	0.0009	0.3335	0.0003	0.0047
L2	2221 (1)	2632 (299)	1770 (442)	413 (151)	90 (90)	0.0005	0.2294	0.0005	0.0078
L4	3051 (2)	1708 (279)	1437 (361)	1057 (628)	310 (345)	0.0007	0.2852	0.0005	0.0075
L6	4617 (4)	2864 (460)	1663 (469)	2161 (1030)	563 (433)	0.0011	0.2465	0.0005	0.0053
L7	4445 (3)	4741 (756)	5453 (1836)	1164 (719)	624 (641)	0.0007	0.3117	0.0004	0.0053
Facility: PTB (manual scoring)									
Lab	0 Gy	0.435 Gy	0.869 Gy	1.74 Gy	3.48 Gy	C	α	SE(C)	SE(α)
L1	1000 (0)	414 (105)	164 (107)	61 (106)	38 (116)	8.5×10^{-8}	0.7737	0.0483	0.0632
L2	1012 (0)	350 (119)	303 (191)	218 (234)	98 (222)	3.0×10^{-6}	0.6743	0.0359	0.0405
L3	1000 (1)	430 (130)	159 (113)	121 (134)	45 (115)	0.0010	0.7096	0.0010	0.0332
L4	1000 (1)	334 (100)	141 (101)	83 (102)	38 (104)	0.0010	0.7464	0.0010	0.0380
L5	1000 (2)	429 (100)	145 (103)	82 (102)	50 (105)	0.0019	0.6494	0.0014	0.0330
L6	1002 (1)	450 (96)	188 (98)	131 (118)	52 (95)	0.0010	0.5290	0.0010	0.0268
L8	250 (0)	500 (145)	450 (323)	300 (379)	200 (570)	1.5×10^{-7}	0.7759	0.0336	0.0330
Facility: PTB (semi-automatic scoring)									
L1	22439 (19)	18706 (1978)	13333 (2928)	9004 (3726)	3297 (2512)	0.0009	0.2369	0.0002	0.0025
L2	6954 (5)	5940 (394)	3906 (697)	1179 (373)	485 (204)	0.0007	0.1708	0.0003	0.0044
L4	3527 (2)	2720 (331)	1997 (531)	1316 (652)	973 (710)	0.0007	0.2582	0.0004	0.0057
L6	3076 (7)	6891 (562)	4344 (563)	5039 (1522)	2432 (989)	0.0043	0.1479	0.0012	0.0027
L7	5232 (5)	5740 (607)	5820 (1361)	3451 (1629)	1331 (913)	0.0010	0.2470	0.0005	0.0039

Table 2: Number of manually and semi-automatically scored metaphases and the number of dicentric chromosomes (in brackets) per dose for test samples with blinded doses irradiated at CINF and PTB.

Facility: CINF (manual scoring; full mode)

Lab	Blind 1 (0 Gy)	Blind 2 (0.6 Gy)	Blind 3 (1.2 Gy)	Blind 4 (2.4 Gy)
L1	514 (1)	141 (103)	85 (109)	38 (111)
L2	500 (1)	250 (165)	200 (212)	60 (121)
L3	513 (0)	215 (106)	123 (126)	53 (108)
L4	500 (5)	174 (100)	83 (101)	41 (101)
L5	500 (1)	358 (197)	165 (187)	84 (194)
L8	200 (0)	197 (127)	399 (517)	200 (545)

Facility: CINF (semi-automatic scoring; full mode)

L1	2481 (3)	3386 (392)	1081 (265)	1217 (676)
L2	2872 (1)	2715 (486)	1514 (603)	560 (306)
L4	1588 (2)	1470 (279)	1587 (623)	1558 (944)
L6	4747 (8)	4197 (796)	4144 (1675)	3008 (2218)
L7	2255 (2)	3241 (685)	1586 (691)	1462 (1144)

Facility: PTB (manual scoring; full mode)

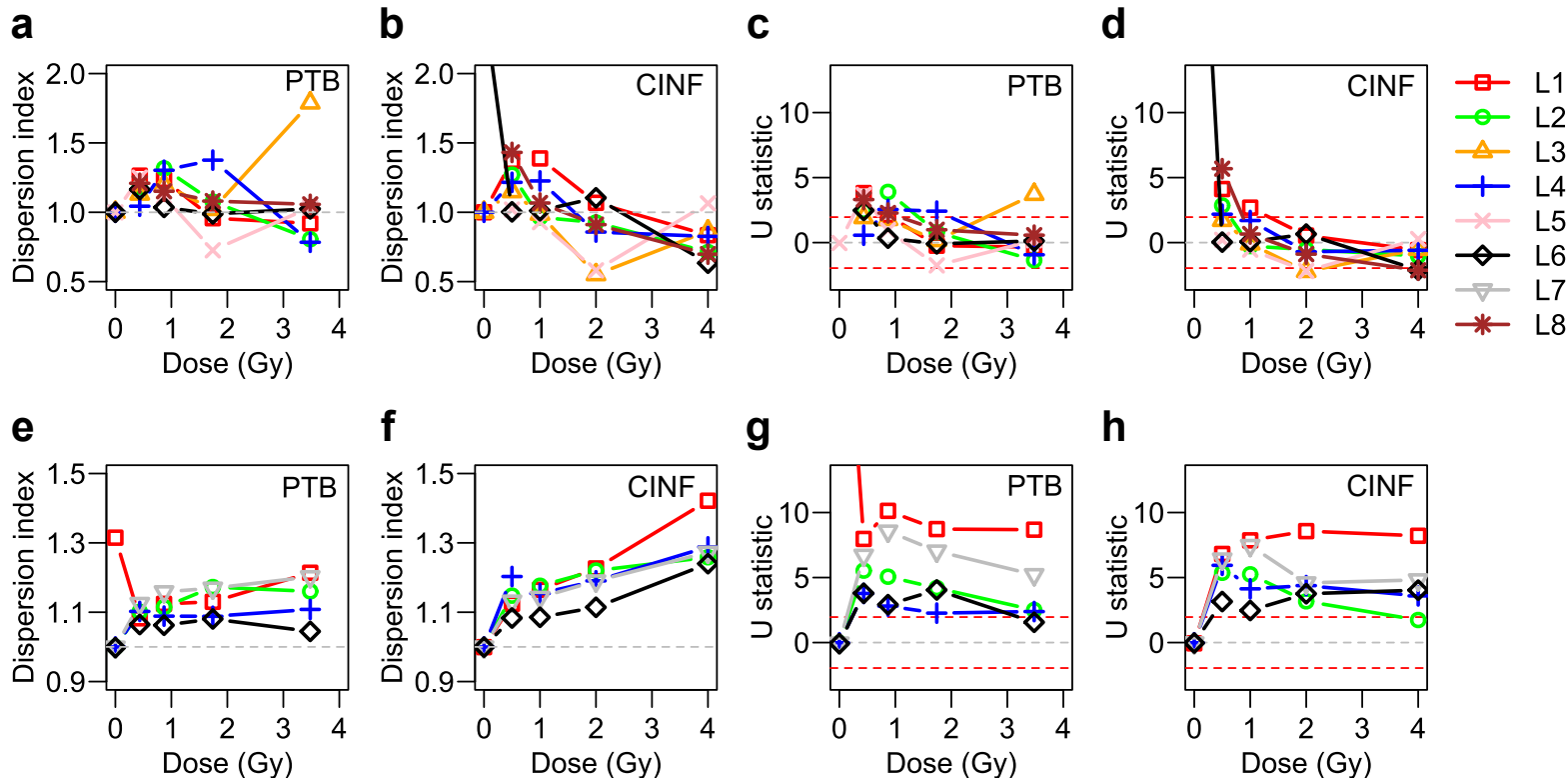
Lab	Blind 1 (0 Gy)	Blind 2 (0.654 Gy)	Blind 3 (1.61 Gy)	Blind 4 (2.23 Gy)
L1	501 (2)	247 (101)	86 (101)	66 (114)
L2	618 (1)	557 (226)	217 (166)	183 (244)
L3	509 (1)	155 (71)	104 (103)	88 (133)
L4	500 (2)	276 (100)	106 (101)	61 (102)
L5	500 (4)	500 (148)	221 (204)	110 (202)
L6	501 (0)	-	123 (113)	78 (127)
L8	150 (0)	267 (105)	199 (212)	148 (249)

Facility: PTB (semi-automatic scoring; full mode)

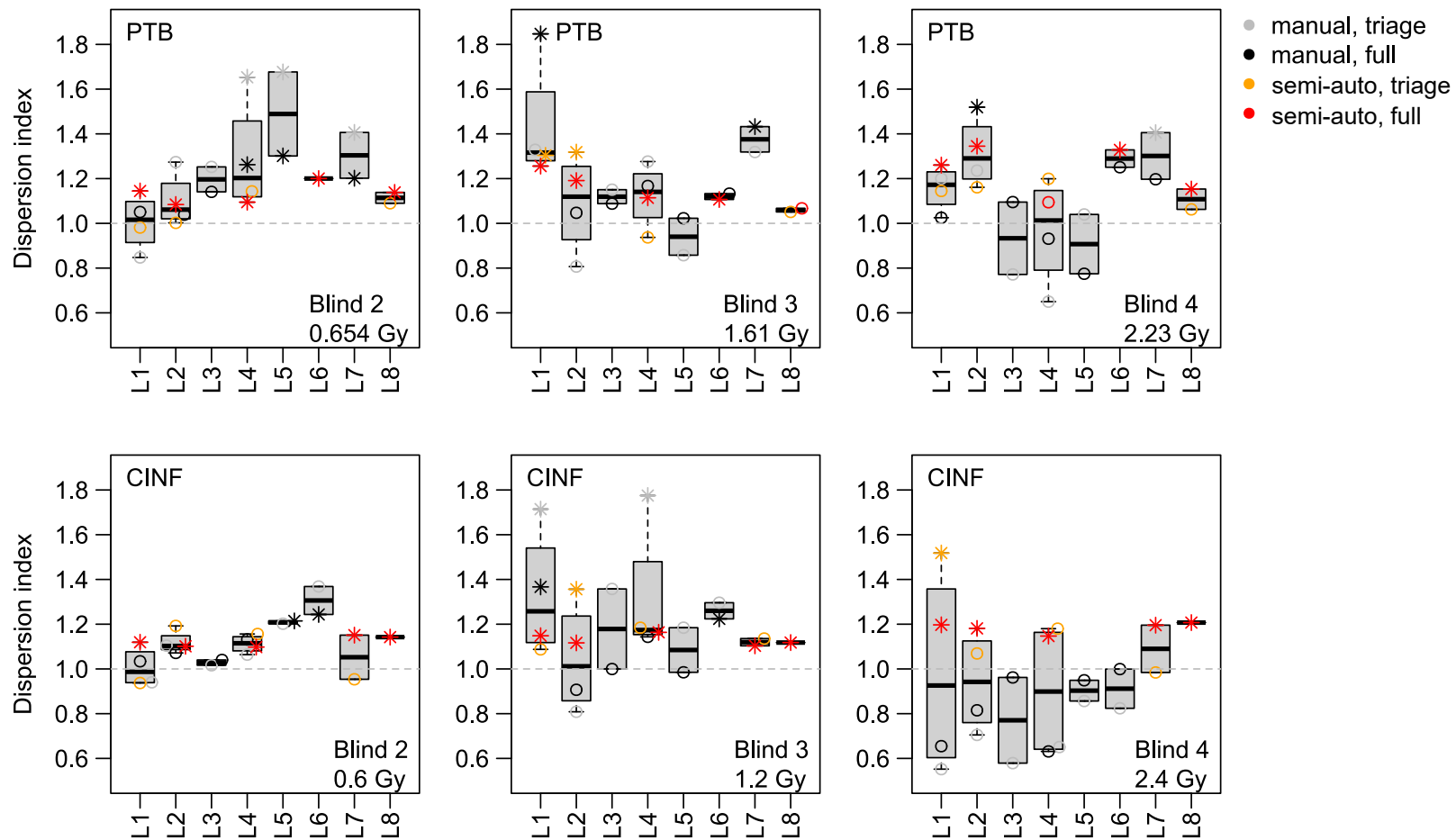
L1	4608 (11)	1978 (251)	992 (282)	1144 (392)
L2	2163 (2)	1894 (256)	621 (143)	555 (223)
L4	1312 (2)	1503 (228)	1142 (365)	818 (403)
L6	2668 (10)	1172 (177)	1515 (533)	158 (94)
L7	3139 (3)	2026 (323)	523 (203)	424 (205)

Table 3. Summary of dose estimates from manual and semi-automatic scoring in full mode for blind samples irradiated at CINF and PTB. The column “Dose” shows the physical reference doses, the column “CV” shows the coefficient of variation, “ δ ” the percentage of results with overdispersion (dispersion index $\delta > 1$), “U” the percentage of results with significant (Papworth’s U test $P < 0.05$) overdispersion and $|\Delta|$ the absolute average difference to the reference dose in mGy. The subsequent columns show the percentage of participants that included the physical reference dose within the estimated 95% confidence interval (CI), or within an interval of ± 0.25 Gy or ± 0.5 Gy, respectively, based on full mode scoring.

Facility: CINF (manual scoring)									
Code	Dose (Gy)	CV	$\delta > 1$ (%)	U > 1.96 (%)	$ \zeta < 2$ (%)	$ \Delta $ (mGy)	95% CI (%)	± 0.25 Gy (%)	± 0.5 Gy (%)
Blind 1	0	-	-	-	-	2	100	100	100
Blind 2	0.6	0.12	100	33	100	56	100	100	100
Blind 3	1.2	0.07	50	33	100	75	100	100	100
Blind 4	2.4	0.09	0	0	100	178	100	83	100
Facility: CINF (semi-automatic scoring)									
Blind 1	0	-	-	-	-	1	100	100	100
Blind 2	0.6	0.27	100	100	20	148	20	80	100
Blind 3	1.2	0.28	100	100	0	361	0	40	80
Blind 4	2.4	0.21	100	100	40	346	40	40	60
Facility: PTB (manual scoring)									
Blind 1	0	-	-	-	-	3	100	100	100
Blind 2	0.654	0.14	100	50	50	118	50	100	100
Blind 3	1.61	0.14	100	29	71	245	71	71	100
Blind 4	2.23	0.17	71	14	71	268	71	57	71
Facility: PTB (semi-automatic scoring)									
Blind 1	0	-	-	-	-	2	80	100	100
Blind 2	0.654	0.26	100	100	40	135	40	80	100
Blind 3	1.61	0.31	100	80	20	367	20	20	80
Blind 4	2.23	0.42	100	80	40	654	40	20	60



Supplementary Figure 1: Dispersion index and U-test statistic for manually and semi-automatically scored calibration curve samples irradiated at PTB and CINF. a&b: Dispersion indices for manually scored calibration curve samples irradiated at PTB and CINF. **c&d:** U-test statistic for manually scored calibration curve samples irradiated at PTB and CINF. **e&f:** Dispersion indices for semi-automatically scored calibration curve samples irradiated at PTB and CINF. **g&h:** U-test statistic for semi-automatically scored calibration curve samples irradiated at PTB and CINF. Dispersion indices >1 indicate overdispersion and $U > 1.96$ indicates significant ($p < 0.05$) overdispersion.



Supplementary Figure 2: Dispersion indices for test samples (Blind 2-4) irradiated at PTB (top row) and CINF (bottom row). Colours indicate manual (gray and black) or semi-automatic scoring (orange and red) in triage (gray and orange) or full mode (black and red); asterisks indicate samples with $U > 1.96$, showing significant ($p < 0.05$) overdispersion.